The Reaction of Tricarbon with Acetylene: An Ab Initio/RRKM Study of the Potential Energy Surface and Product Branching Ratios†

Alexander M. Mebel,*,‡ Gap-Sue Kim,§ Vadim V. Kislov,‡,|| and Ralf I. Kaiser+

Department of Chemistry and Biochemistry, Florida International University, Miami, Florida 33199, School of Chemistry, Seoul National University, Seoul 151-147, Korea, and Department of Chemistry, University of Hawai'i at Manoa, Honolulu, Hawaii 96822-2275

Received: December 29, 2006; In Final Form: February 15, 2007

Ab initio calculations of the potential energy surface for the $C_3(^1\Sigma_g^+)$ + $C_2H_2(^1\Sigma_g^+)$ reaction have been performed at the RCCSD(T)/cc-pVQZ//B3LYP/6-311G(d,p) + ZPE[B3LYP/6-311G(d,p)] level with extrapolation to the complete basis set limit for key intermediates and products. These calculations have been followed by statistical calculations of reaction rate constants and product branching ratios. The results show the reaction to begin with the formation of the 3-(didehydrovinylidene)cyclopropene intermediate **i1** or five-member ring isomer **i7** with the entrance barriers of 7.6 and 13.8 kcal/mol, respectively. **i1** rearranges to the other C_5H_2 isomers, including ethynylpropadienylidene **i2**, singlet pentadiynylidene **i3**, pentatetraenylidene **i4**, ethynylcyclopropenylidene **i5**, and four- and five-member ring structures **i6**, **i7**, and **i8** by ring-closure and ring-opening processes and hydrogen migrations. **i2**, **i3**, and **i4** lose a hydrogen atom to produce the most stable linear isomer of C_5H with the overall reaction endothermicity of ∼24 kcal/mol. H elimination from **i5** leads to the formation of the cyclic C_5H isomer, HC_2C_3, + H, 27 kcal/ mol above C_3 + C_2H_2. 1,1-H_2 loss from **i4** results in the linear pentacarbon C_5 + H_2 products endothermic by 4 kcal/mol. The H elimination pathways occur without exit barriers, whereas the H_2 loss from **i4** proceeds via a tight transition state 26.4 kcal/mol above the reactants. The characteristic energy threshold for the reaction under single collision conditions is predicted be in the range of ∼24 kcal/mol. Product branching ratios obtained by solving kinetic equations with individual rate constants calculated using RRKM and VTST theories for collision energies between 25 and 35 kcal/mol show that *l*-C_5H + H are the dominant reaction products, whereas HC_2C_3 + H and *l*-C_5 + H_2 are minor products with branching ratios not exceeding 2.5% and 0.7%, respectively. The ethynylcyclopropenylidene isomer **i5** is calculated to be the most stable C_5H_2 species, more favorable than triplet pentadiynylidene **i3t** by ∼2 kcal/mol.

Introduction

The reactions of the bare carbon clusters C_2 (dicarbon) and C_3 (tricarbon) with unsaturated hydrocarbons are of importance in combustion processes, where they contribute to the formation of resonantly stabilized free radicals (RSFRs) playing an important role in the formation of polycyclic aromatic hydrocarbons (PAHs),[1−4] and in the interstellar medium, where they are involved in the chemical evolution of extraterrestrial environments such as molecular clouds and circumstellar envelopes of dying carbon stars.[5,6] The reactions of dicarbon with unsaturated hydrocarbons have been recently established to proceed mostly by the C_2 for H exchange channel, C_2 + $C_nH_m \rightarrow C_{n+2}H_{m-1}$ + H.[4,6−10] Experimental crossed molecular beams studies combined with theoretical calculations of potential energy surfaces (PES) for the reactions of C_2 with acetylene,[7] ethylene,[8] C_3H_4 isomers allene and methylacetylene,[9] and benzene[10] showed that these reactions produce a variety of RSFRs, such as 1,3-butadiynyl [$C_4H(X^2\Sigma^+)$ HCCCC], 1-butene-3-yne-2-yl [i-$C_4H_3(X^2A')$ H_2CCCCH], 2,4-pentadiynyl-1 [$C_5H_3(X^2B_1)$ $HCCCCCH_2$], 1,4-pentadiynyl-3 [$C_5H_3(X^2B_1)$ HCCCHCCH], and phenylethynyl [$C_6H_5C_2(^2A')$] radicals, respectively, under single collision conditions. The reactions of tricarbon with unsaturated hydrocarbon have not been thoroughly investigated until now. By a simple analogy with the C_2 reactions one can expect that the C_3 for H exchange channel, C_3 + $C_nH_m \rightarrow C_{n+3}H_{m-1}$ + H, should be important. Indeed, a crossed molecular beams study of the C_3 reaction with C_2H_4 combined with quantum chemical calculations of the singlet C_5H_4 potential energy surface (PES) showed that the $HCCCCCH_2$ and HCCCHCCH isomers of the C_5H_3 radical are the major reaction products.[4,9a] The PES calculations for C_3 + C_2H_4 revealed that this reaction exhibits significant entrance barriers in the range of 6−11 kcal/mol,[4] on the contrary to the C_2 reactions with unsaturated hydrocarbons, which proceed without activation. A recent experimental investigation of tricarbon reactions with allene and methylacetylene by Kaiser and co-workers[11] demonstrated that they also involve the C_3 for H exchange channel and the dominant product observed was 1-hexene-3,4-diynyl-2 radical (C_6H_3; $H_2CCCCCCH$). The C_3 + C_3H_4 reactions exhibited characteristic threshold energies of 10−12 kcal/mol.[11]

In this view, we can anticipate that the reaction of C_3 with acetylene taking place on the C_5H_2 PES should lead predominantly to the C_5H + H reaction products, although other

† Part of the special issue "M. C. Lin Festschrift".

* Corresponding author. Fax: +1-305-348-3772. E-mail address: mebela@fiu.edu.

‡ Florida International University.

§ Seoul National University.

|| Permanent address: Institute of Solution Chemistry of Russian Academy of Sciences, Akademicheskaya St., 1, Ivanovo, 153045, Russia.

\+ Florida International University.

10.1021/jp0690300 CCC: $37.00 © 2007 American Chemical Society
Published on Web 03/29/2007

products, such as $C_5 + H_2$, $C_3H + C_2H$, or $C_3H_2 + C_2$ cannot be a priori excluded. C_5H_2 isomers were a subject of several experimental and theoretical studies because of the possibility that compounds derived from stable C_3H_2 species by addition of carbon chains might be stable[12,13] and the fact that highly unsaturated carbenes with a large ratio of carbon to hydrogen are widely distributed in interstellar and circumstellar environments.[14] Three C_5H_2 isomers have been identified experimentally, including the cumulene carbene pentatetraenylidene,[15] the ring-chain compound ethynylcyclopropenylidene,[16] and the triplet pentadiynylidene.[17] Also, several theoretical investigations of C_5H_2 have been reported in the literature.[13,18−21] The most detailed of them up to now is a coupled cluster study by Seburg et al.,[21] who calculated geometries, vibrational frequencies, and relative energies of five different local minima on the C_5H_2 PES. However, rearrangement and decomposition pathways of these structures have not been mapped out. The potential product of the $C_3 + C_2H_2$ reaction, the C_5H radical, which is a member of the C_nH series of carbon chain radicals in an unusual class of non-terrestrial molecules,[22] had been identified in the interstellar medium using radioastronomical techniques by Cernicharo et al.[23] and later had been detected in a laboratory by Gottlieb et al.[24] Its electronic spectra were consequently measured my Ding et al. using the mass-selective resonant two-color two-photon ionization spectroscopy.[25] High-level theoretical studies of structure and energetics of C_5H isomers have been reported by Crawford et al.[26] However, the formation mechanism of C_5H either in the interstellar medium or in combustion flames has not been well understood so far.

In the present paper, we continue our systematic ab initio and density functional calculations of PESs and reaction mechanisms of dicarbon and tricarbon with unsaturated hydrocarbons and investigate the $C_3 + C_2H_2$ reaction, which may lead to the production of C_5H. Our goal is to map out all possible reaction pathways, starting from the formation of an initial C_5H_2 adduct and leading to various products through isomerization and decomposition of C_5H_2 intermediates and to predict product branching ratios depending on the reactive collision energy employing statistical theories. Our theoretical studies are complementally to experimental crossed molecular beams investigations of the $C_3 + C_2H_2$ reaction under single collision conditions, which are currently underway in Kaiser's group.

Computational Methods

The geometries of the reactants, products, intermediates, and transition states in the $C_3(^1\Sigma_g^+) + C_2H_2(^1\Sigma_g^+)$ reaction have been optimized at the hybrid density functional B3LYP level of theory[27,28] with the 6-311G(d,p) basis set. Vibrational frequencies have been calculated at the same level and were used for characterization of the stationary points as local minima and transition states, to compute zero-point energy corrections (ZPE), and for statistical calculations of rate constants for individual reactions steps. All connections between intermediates and transition states have been confirmed by intrinsic reaction coordinate (IRC) calculations.[29] Relative energies of various species were refined at the coupled cluster RCCSD(T) level[30] with Dunning's correlation consistent cc-pVQZ basis set.[31] The RCCSD(T)/cc-pVQZ//B3LYP/6-311G(d,p) + ZPE[B3LYP/6-311G(d,p)] calculational approach is expected to provide accuracies of 1−2 kcal/mol for relative energies of various stationary points on PES, including transition states.[32] For the reaction products and key C_5H_2 intermediates, we additionally carried out RCCSD(T) calculations with Dunning's cc-pVDZ, cc-pVTZ, and cc-pV5Z basis sets[31] and extrapolated their total energies to the complete basis set (CBS) limit using the procedure suggested by Peterson and Dunning.[33] The GAUSSIAN 98[34] and MOLPRO 2002[35] program packages were employed for the calculations.

We used RRKM theory for computations of rate constants of individual reaction steps.[36−38] The calculations were performed with different values of the internal energy E_{int} computed as a sum of the energy of chemical activation (the relative energy of an intermediate or a transition state with respect to the initial reactants) and the collision energy E_c. For the reaction channels, which do not exhibit exit barriers, such as H atom eliminations from various C_5H_2 intermediates occurring by a cleavage of single C−H bonds, we applied the microcanonical variational transition state theory (VTST)[38] and thus determined variational transition states and rate constants. We used the following procedure for the VTST calculations. At first, we calculated a series of energies at different values of the reaction coordinate in question, i.e., the length of the C−H bond being cleaved. To obtain these energies, we performed partial UB3LYP/6-31G** geometry optimization with fixed values of the reaction coordinate and all other geometric parameters being optimized. The unrestricted UB3LYP theoretical level was used for these calculations because VTSs are typically observed for single-bond cleavage processes, in which a closed-shell singlet wave function of a reactant converts into an open-shell singlet (doublet + doublet) wave function of products. Then we calculated 3N-7 vibrational frequencies projecting the reaction coordinate out. The UB3LYP/6-311G** energies were multiplied by a scaling factor in order to match them to the RCCSD(T)/cc-pVQZ energies of the final dissociation products.

Finally, first-order kinetic equations were solved utilizing the steady-state approximation and using microcanonical rate constants obtained from the RRKM and VTST calculations. Only a single total-energy level was considered throughout, as for single-collision crossed-beam conditions.

Results and Discussion

Potential Energy Surface of the $C_3 + C_2H_2$ Reaction. Optimized geometries of various intermediates and transition states involved in the reaction of tricarbon with acetylene are illustrated in Figures 1 and 2, respectively, and their molecular parameters (rotational constants and vibrational frequencies) are given in Table 1. The computed profile of PES from the reactants to possible products is shown in Figure 3, where part a shows pathways involving chain and three-member ring C_5H_2 isomers and part b illustrates reaction channels via five- and four-member ring and bicyclic structures.

The reaction starts from the formation of a weakly bound planar $C_3...C_2H_2$ complex **i0**. The shortest C−C distance between the C_3 and C_2H_2 fragments in the complex is 3.157 Å and the binding energy is only 0.9 kcal/mol. As the tricarbon molecule approaches closer to acetylene to attach to the in-plane π bond of C_2H_2, a barrier of 7.6 kcal/mol (with respect to the initial reactants) has to be overcome. In the corresponding transition state TS01, the shortest C−C distance between the fragments decreases to 2.045 Å, and the geometry remains planar. After the barrier is cleared, the C_3 fragment moves into a position above the center of the acetylenic C−C bond and two new equivalent carbon−carbon bonds are created. This leads to the formation of the three-member ring adduct **i1**, 3-(didehydrovinylidene)cyclopropene, which has C_{2v} symmetry. The C_5H_2 intermediate **i1** has electronic structure similar to that of cyclopropenylidene *c*-C_3H_2, with the lone pair on the hydrogen-free C atom replaced by a double C═C bond and the carbene

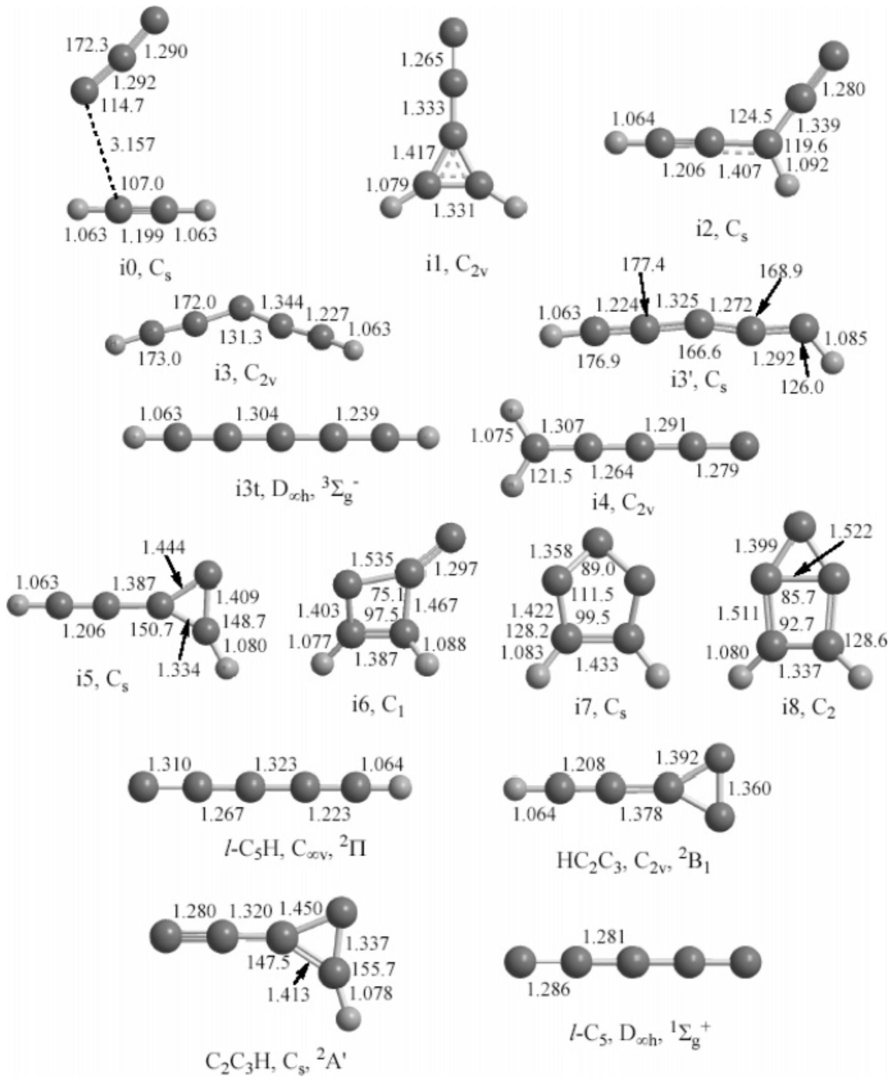

Figure 1. Geometric structures of C_5H_2 intermediates and C_5H and C_5 products of the $C_3 + C_2H_2$ reaction optimized at the B3LYP/6-311G(d,p) level. Bond lengths are given in angstrom and bond angles in degrees.

position shifted to the terminal carbon. **i1** resides 54.5 kcal/mol lower in energy than $C_3 + C_2H_2$. It is worth noting that the C_{2v}-symmetric pathway for the addition of C_3 to acetylene to form **i1** is forbidden; the separated reactants have 11 a_1, 2 b_1, and 3 b_2 occupied orbitals within C_{2v} symmetry, whereas the product has 10 a_1, 2 b_1, and 4 b_2 occupied orbitals. Therefore, the attacking tricarbon molecule has to slide from the side in order to attach to the in-plane π bond of C_2H_2; only C_s symmetry is maintained in this case.

Alternatively, the $C_3 + C_2H_2$ reaction can begin with the tricarbon molecule approaching acetylene in a parallel fashion. In this case, the attacking C_3 fragment eventually loses its linearity and two terminal carbon atoms of tricarbon form two new C−C bonds with acetylenic carbons. This pathway leads to the production of the five-member ring intermediate **i7** residing 22.9 kcal/mol below the reactants via a 13.8 kcal/mol barrier at a planar transition state TS07. Because the calculated barrier at TS07 is 6.2 kcal/mol higher than that at TS01, we expect the $C_3 + C_2H_2 \rightarrow$ **i7** initial reaction channel to be less significant than $C_3 + C_2H_2 \rightarrow$ **i1**.

The further fate of the adduct **i1** is threefold. First, it can undergo a 1,2-H shift from a CH group in the three-member ring to the central carbon atom accompanied with a cleavage of the opposite HC−C bond in the cycle. This process takes place via a planar transition state TS12 overcoming a barrier of 64.4 kcal/mol (9.9 kcal/mol above the initial reactants) and leads to the chain intermediate **i2**, ethynylpropadienylidene HC-CCHCC. **i2** also possesses C_s symmetry and resides 58.7 kcal/mol below $C_3 + C_2H_2$ being 4.2 kcal/mol more stable than the cyclic isomer **i1**. The second possible pathway is hydrogen migration from CH to the neighboring CH group also accompanied by the ring opening, which makes the newly formed CH_2 group terminal. This process leads to the formation of the H_2CCCCC intermediate **i4** (pentatetraenylidene) residing 60.3 kcal/mol below the initial reactants. The barrier for such H shift is high, 72.0 kcal/mol, and the corresponding transition state TS14 lies 17.5 kcal/mol above $C_3 + C_2H_2$. The third alternative is expansion of the three-member ring in **i1** to a four-member ring to produce isomer **i6** via transition state TS16 overcoming a barrier of 60.6 kcal/mol. **i6** has no symmetry and lies only 17.2 kcal/mol lower in energy than the initial reactants. Elimination of a hydrogen atom from **i1** would lead to a three-member ring isomer of C_5H, C_2-C_3H, with the H atom and C_2 group attached to two different carbons in the ring. However, according to earlier CCSD(T)/TZ2P calculations by Crawford et al.,[26] this isomer lies 24.1 kcal/mol higher in energy than the most stable linear C_5H configuration. Our calculations show that the C_2-C_3H + H products lie 50.4 kcal/mol above $C_3 + C_2H_2$, which indicates that their formation is highly unfavorable and can be excluded from the present consideration.

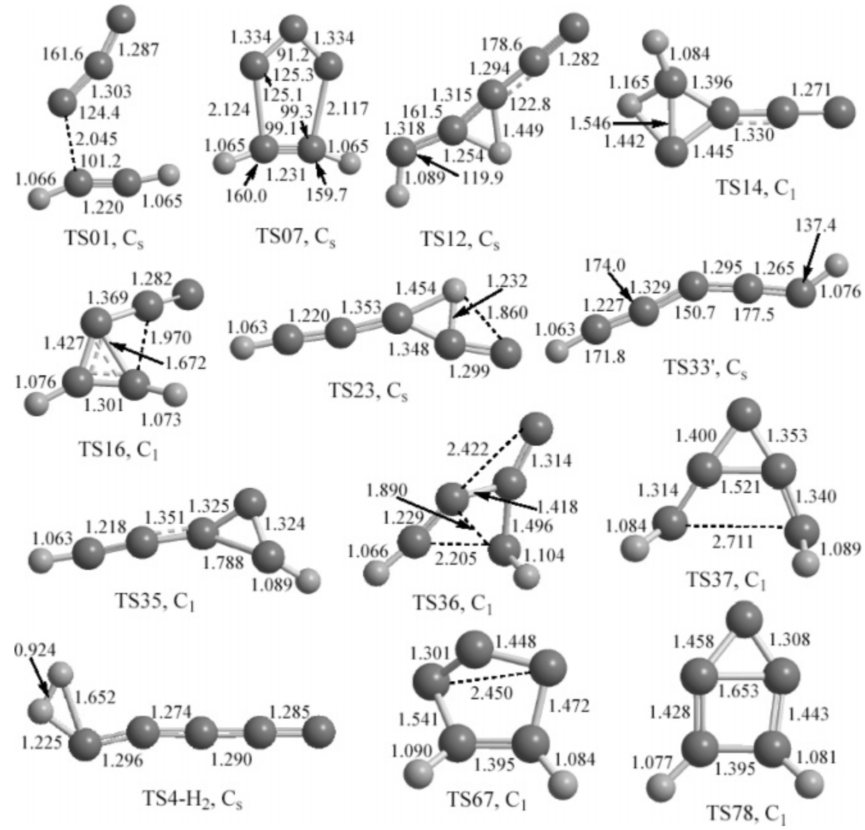

Figure 2. Geometric structures of transition states on the C_5H_2 potential energy surface involved in the $C_3 + C_2H_2$ reaction optimized at the B3LYP/6-311G(d,p) level. Bond lengths are given in angstrom and bond angles in degrees.

Two distinct reaction pathways are possible starting from intermediate **i2**. Hydrogen elimination from the central C atom leads to the *l*-$C_5H(^2\Pi)$ + H products, which lie 24.4 kcal/mol above the initial reactants. The cleavage of the single C−H bond in this case occurs without an exit barrier. On the other hand, a 1,3-H shift from the central carbon to the hydrogen-less end of the molecule leads to the structure HCCCCCH overcoming a barrier of 69.2 kcal/mol. The corresponding transition state TS23 resides 11.2 kcal/mol higher in energy than $C_3 + C_2H_2$. IRC calculations in the forward direction from TS23 converge to the C_s-symmetric isomer **i3′**, 56.7 kcal/mol below the reactants. However, **i3′** is only a metastable intermediate, which should rapidly rearrange to the more stable isomer **i3** of C_{2v} symmetry via a barrier of only 0.2 kcal/mol. Singlet pentadiynylidene **i3** is calculated to be 1.7 kcal/mol more stable than **i3′** and nearly isoergic with **i2**. The singlet electronic state is not the ground state for the HCCCCCH configuration; a linear **i3t**($^3\Sigma_g^-$) structure in the triplet state is 13.8 kcal/mol more stable than **i3**. H loss from the terminal carbon atom in **i2** is not anticipated to be favorable because the C_2CHC_2 isomer of the C_5H radical was earlier calculated to lie 45−49 kcal/mol higher in energy than the most stable *l*-C_5H structure.[26]

i3 can also be produced from the four-member ring intermediate **i6** either directly or via a two-step mechanism. In the direct process, the rupture of the HC−CH bond in the ring is accompanied by the insertion of the out-of-ring C atom into the C−C bond opposite to HC−CH. The corresponding transition state TS36 is 20.5 kcal/mol higher in energy than C_3 + C_2H_2. The two-step rearrangement is slightly more favorable and involves first ring expansion in **i6**, leading to the five-member ring intermediate **i7** via a barrier of 15.4 kcal/mol, followed by the cleavage of the HC−CH bond in **i7**, resulting in **i3** over a higher 36.6 kcal/mol barrier. The rate-determining transition state TS37 for the **i6** → **i7** → **i3** pathway lies 13.7 kcal/mol above the reactants, i.e., 6.8 kcal/mol lower than TS36 for the **i6** → **i3** process. The nonplanar but C_s-symmetric structure **i7** resides 5.7 and 22.9 kcal/mol lower in energy than **i6** and the reactants, respectively.

The HCCCCCH intermediate **i3** can undergo a hydrogen loss to produce *l*-C_5H. This process is endothermic by 82.8 kcal/mol and takes place without an exit barrier. Alternatively, ring closure in **i3** results in the most stable singlet C_5H_2 isomer **i5**, planar ethynylcyclopropenylidene, residing 73.7 kcal/mol below $C_3 + C_2H_2$. The barrier at TS35 is relatively low, 42.2 kcal/mol, with the transition state lying 16.2 kcal/mol lower in energy than the initial reactants. H elimination from a carbon atom included in the three-member ring of **i5** gives the second most stable C_5H isomer, HC_2C_3 (C_{2v}, $^2B_1$), which lies 28.0 kcal/mol above the reactants. The H loss from the terminal carbon atom in ethynylcyclopropenylidene leading to C_2C_3H is much less favorable and is not expected to be competitive. Two decomposition pathways are found for pentatetraenylidene **i4**, which can be produced from **i1**. H loss in **i4**, endothermic by 84.7 kcal/mol, yields *l*-C_5H + H without an exit barrier. On the other hand, the 1,1-H_2 elimination giving $C_5(^1\Sigma_g^+) + H_2$ is much less endothermic (by 56.5 kcal/mol) but is accompanied with a high barrier of 86.7 kcal/ mol at TS4-H_2. The structure **i7** can isomerize further to a bicyclic intermediate **i8** of C_2 symmetry. The energies of **i7** and **i8** are close to one another and they are separated by a low barrier of 1.1−2.2 kcal/mol. Both **i7** and **i8** are not expected to directly eliminate a hydrogen atom, because no low-lying five-member ring or bicyclic isomers of the C_5H radical have been found.

In summary, we found nine different isomers on the singlet C_5H_2 PES. The most stable of them is ethynylcyclopropenylidene **i5**, which is calculated to lie 1.5 kcal/ mol lower in

TABLE 1: Molecular Parameters of Various Local Minima and Transition States on the C_5H_2 Potential Energy Surface Calculated at the B3LYP/6-311G(d,p) Level of Theory

species	rotational constants (GHz)	harmonic vibrational frequencies (cm^{-1}) and infrared intensities (km/mol, in parentheses)
i0	13.282, 1.994, 1.734	28 (2.7), 43 (0.2), 52 (4.3), 95 (1.1), 123 (11.8), 168 (9.2), 651 (0.5), 653 (1.9), 773 (136.8), 778 (88.9), 1244 (0.4), 2061 (13.8)
i1	32.172, 3.521, 3.173	156 (1.0), 174 (0.2), 464 (10.0), 499 (0.1), 738 (0.3), 772 (50.4), 925 (11.7), 957 (0), 967 (2.1), 1113 (16.9), 1466 (151.8), 1679 (27.0), 2088 (921.5), 3233 (4.9), 3272 (9.4)
i2	32.341, 2.858, 2.626	136 (3.6), 222 (1.8), 311 (2.0), 317 (15.2), 592 (7.6), 670 (46.8), 734 (29.3), 895 (3.3), 968 (40.4), 1169 (9.4), 1402 (4.3), 2034 (697.5), 2189 (79.7), 3088 (1.7), 3466 (67.0)
i3	66.772, 2.560, 2.465	109 (0.7), 195 (63.0), 243 (144.6), 315 (2.6), 330 (0), 463 (0.0), 539 (0.3), 824 (38.2), 830 (0), 837 (8.5), 1409 (25.5), 1973 (60.0), 2048 (3.3), 3463 (160.4), 3466 (24.1)
i3	517.700, 2.307, 2.297	53 (6.6), 182 (16.4), 252 (97.8), 333 (0.0), 406 (91.9), 457 (4.6), 621 (252.6), 643 (36.7), 780 (1.9), 810 (13.1), 1482 (1.0), 1903 (9.5), 2071 (17.9), 3199 (2.2), 3467 (135.1)
i3t	2.274	128 (4.2), 128 (4.2), 396 (0), 396 (0), 414 (25.7), 414 (25.7), 448 (0), 448 (0), 461 (70.4), 461 (70.4), 766 (0), 1569 (2.5), 1735 (7.3), 1964 (0), 3458 (219.1), 3465 (0)
i4	291.771, 2.311, 2.293	130 (2.6), 144 (0.0), 267 (7.3), 282 (8.1), 467 (1.8), 611 (5.7), 769 (0.1), 970 (32.3), 1032 (0.0), 1370 (9.3), 1512 (9.8), 1978 (204.8), 2214 (806.7), 3101 (2.5), 3178 (0.3)
i5	34.825, 3.428, 3.121	199 (6.0), 216 (1.1), 528 (2.2), 539 (1.9), 608 (56.0), 704 (1.0), 753 (28.3), 897 (17.4), 943 (3.6), 1096 (6.4), 1274 (34.2), 1722 (34.5), 2195 (5.8), 3236 (0.3), 3471 (87.0)
i6	18.934, 5.520, 4.558	202 (13.2), 250 (0.2), 539 (16.9), 630 (26.6), 670 (5.1), 809 (31.9), 861 (50.1), 984 (4.6), 1037 (4.7), 1172 (6.4), 1272 (9.6), 1434 (13.8), 1794 (216.7), 3136 (3.3), 3268 (3.1)
i7	12.482, 9.574, 5.735	315 (51.7), 391 (7.7), 669 (16.9), 790 (52.3), 853 (29.7), 877 (14.8), 930 (99.9), 1013 (29.6), 1177 (23.2), 1184 (7.1), 1251 (109.7), 1318 (13.4), 1358 (10.1), 3196 (1.9), 3212 (3.3)
i8	17.383, 7.266, 5.180	309 (53.2), 346 (34.9), 478 (22.6), 584 (35.1), 658 (0.0), 784 (31.5), 829 (33.1), 973 (1.3), 1038 (38.5), 1108 (2.1), 1223 (18.7), 1516 (2.8), 1571 (7.1), 3212 (0.1), 3242 (0.1)
TS01	18.316, 3.066, 2.626	344*i*, 86, 133, 212, 246, 422, 641, 686, 788, 895, 1263, 1951, 2055, 3392, 3478
TS07	13.976, 5.233, 3.807	462*i*, 95, 160, 368, 409, 542, 731, 758, 786, 823, 1464, 1473, 1892, 3386, 3460
TS12	193.447, 2.381, 2.352	1048*i*, 141, 158, 287, 375, 601, 637, 756, 857, 926, 1381, 1831, 2098, 2133, 3161
TS14	28.171, 3.642, 3.256	700*i*, 164, 176, 302, 470, 524, 767, 813, 1019, 1046, 1350, 1588, 2074, 2552, 3198
TS16	21.134, 4.795, 4.145	690*i*, 187, 267, 457, 514, 547, 724, 906, 931, 1069, 1182, 1649, 1861, 3275, 3324
TS23	101.637, 2.479, 2.420	1678i, 144, 153, 283, 342, 397, 425, 504, 800, 800, 1370, 1799, 2070, 2333, 3465
TS33	146.728, 2.399, 2.361	81i, 206, 297, 332, 362, 460, 504, 728, 810, 823, 1502, 1884, 2051, 3295, 3462
TS35	38.243, 3.183, 2.999	1021*i*, 134, 187, 391, 455, 468, 662, 802, 843, 942, 1429, 1642, 2086, 3122, 3468
TS36	16.102, 5.174, 3.987	268*i*, 163, 250, 462, 511, 581, 760, 812, 965, 994, 1121, 1713, 2017, 2976, 3443
TS37	9.975, 7.672, 4.441	392*i*, 236, 357, 394, 454, 502, 767, 834, 869, 919, 1109, 1393, 1770, 3152, 3214
TS4−H2	186.845, 2.318, 2.289	1064*i*, 128, 142, 273, 282, 502, 561, 605, 750, 787, 1419, 1700, 1995, 2187, 2503
TS67	12.417, 9.055, 5.615	534*i*, 403, 597, 656, 807, 822, 850, 993, 1039, 1103, 1289, 1339, 1518, 3121, 3191
TS78	15.677, 8.029, 5.444	340*i*, 301, 533, 638, 650, 734, 810, 997, 1090, 1127, 1259, 1343, 1674, 3211, 3259

energy than triplet pentadiynylidene **i3t** at the CCSD(T)/cc-pVQZ// B3LYP/6-311G(d,p) + ZPE[B3LYP/6-311G(d,p)] level. This result somewhat differ from that obtained in CCSD(T)/cc-pVTZ calculations by Seburg et al.[21] who found a 2.0 kcal/mol energy difference between the two isomers, but in favor of triplet pentadiynylidene. CCSD(T)/CBS calculations confirm the preference of singlet ethynylcyclopropenylidene **i5** over triplet pentadiynylidene and give their energy difference as 2.3 kcal/mol. Noteworthy, this result does not change significantly when we use CCSD/DZP calculated frequencies[21] instead of B3LYP/6-311G(d,p) frequencies to evaluate ZPE corrections. The **i3t** structure is then slightly stabilized (by 0.5 kcal/mol), but **i5** remains more favorable by 1.8 kcal/mol. All other singlet isomers appear to be less stable than **i3t**. For instance, pentatetraenylidene **i4** lies 11.9 kcal/mol above **i3t** (compare with 13.8 kcal/mol obtained by Seburg et al.[21]), whereas ethynylpropadienylidene **i2** and 3-(didehydrovinylidene)cyclopropene **i1** are less stable than **i3t** by 13.5 and 17.7 kcal/mol, respectively (16.8 and 21.1 kcal/ mol in earlier calculations[21]). It should be noted that the present B3LYP/ 6-311G(d,p) optimized geometries of C_5H_2 isomers are in close agreement with the CCSD(T)/cc-pVTZ structures calculated by Seburg et al.;[21] the difference in bond lengths and bond angles do not exceed 0.01 Å and 1°, respectively. For the C_5H isomers, the agreement of our B3LYP results with the CCSD/TZ2P geometries reported by Crawford et al.[26] is also close, normally within 0.01 Å and 1°, with the largest deviation in the bond lengths not exceeding 0.028 Å. As compared to the study by Seburg et al.,[21] five additional C_5H_2 isomers are found here: singlet pentatetraenylidenes **i3** and **i3′** (13.8 and 15.5 kcal/mol above **i3t**, respectively) as well as cyclic structure **i6** (55.0 kcal/mol), **i7** (49.3 kcal/mol), and **i8** (48.8 kcal/ mol).

In terms of the energetics, the most favorable mechanisms of the $C_3 + C_2H_2$ reaction are the following: $C_3 + C_2H_2 \rightarrow$ **i0** $\rightarrow$ **i1** $\rightarrow$ **i2** $\rightarrow$ *l*-C_5H + H, ... **i2** $\rightarrow$ **i3** $\rightarrow$ *l*-C_5H + H, ... **i3** $\rightarrow$ **i5** $\rightarrow$ HC_2C_3 + H, ... **i1** $\rightarrow$ **i6** $\rightarrow$ **i7** $\rightarrow$ **i3** $\rightarrow$ ..., $C_3 + C_2H_2 \rightarrow$ **i7** $\rightarrow$ **i3** $\rightarrow$ ..., ... **i1** $\rightarrow$ **i4** $\rightarrow$ *l*-C_5H + H, and ... **i4** $\rightarrow$ *l*-C_5 + H_2. At out best CCSD(T)/ CBS level, the C_5H + H reaction products are calculated to be endothermic by 24.5 and 27.2 kcal/mol for the linear and cyclic HC_2C_3 isomers, respectively. The *l*-C_5 + H_2 products are significantly less endothermic, only by 4.0 kcal/mol, however, the H_2 elimination involves a high exit barrier, with the transition state lying 26.4 kcal/ mol above the initial reactants. The $C_3 + C_2H_2$ reaction exhibits a sizable entrance barrier of 7.6 kcal/mol. However, this barrier and the isomerization barriers on the singet C_5H_2 PES, which are located in the range of 10−20 kcal/mol relative to $C_3 + C_2H_2$, have lower energies as compared to the C_5H + H products and the exit transition state leading to *l*-C_5 + H_2. This indicates that apparently the last reaction steps should be rate-determining for the formation of C_5H + H and C_5 + H_2. Since the relative energies of *l*-C_5H + H, HC_2C_3 + H, and the transition state for H_2 elimination are rather close to each other (within a 2.7 kcal/mol range), rate constant calculations are needed to predict relative yields of these reaction products. It should be noted that dissociation of C_5H_2 to other, heavier fragments is not expected to be competitive with the H and H_2 losses because of the unfavorable energetics. In particular, the *l*-C_3H + C_2H, *c*-C_3H + C_2H, and *c*-C_3H_2 + $C_2(^1\Sigma_g^+)$ products are calculated to lie respectively 58.1, 55.6, and 64.3 kcal/mol higher in energy

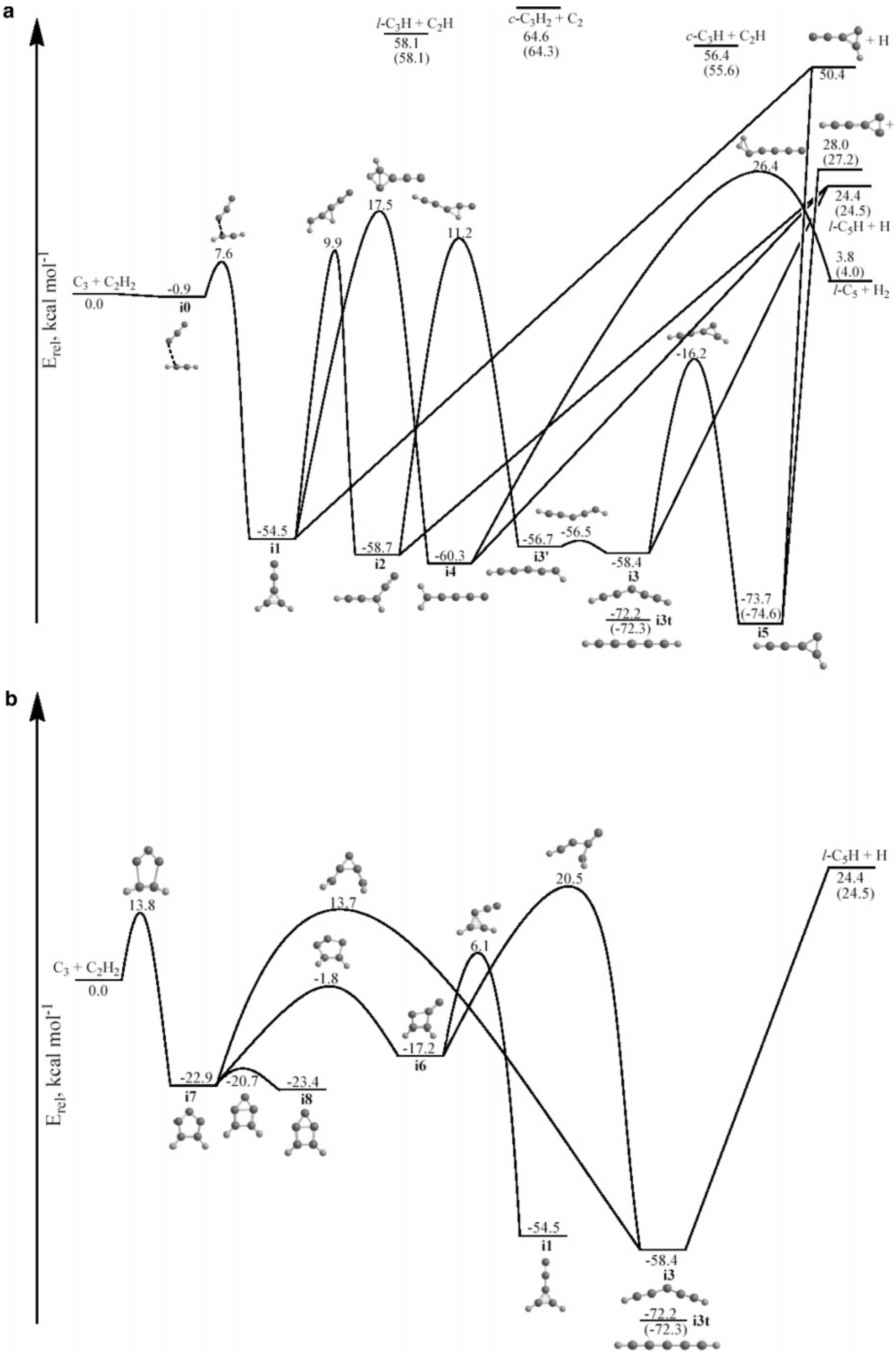

Figure 3. Potential energy diagram of the $C_3 + C_2H_2$ reaction calculated at the RCCSD(T)/cc-pVQZ//B3LYP/6-311G(d,p) + ZPE[B3LYP/6-311G(d,p)] level: (a) pathways involving chain and three-member ring intermediates; (b) pathways involving five-and four-member ring and bicyclic structures. All relative energies are given in kcal/mol. The numbers in parenthesis show RCCSD(T) relative energies extrapolated to the complete basis set limit.

TABLE 2: Unimolecular Rate Constants (s^{-1}) for Isomerization and Dissociation of Singlet C_5H_2 Isomers Calculated for Collision Energies of 25−35 kcal/mol

reaction	σ^a	E_c = 2 5.0	E_c = 26.0	E_c = 27.0	E_c = 28.0	E_c = 29.0	E_c = 30.0	E_c = 31.0	E_c = 32.0	E_c = 33.0	E_c = 34.0	E_c = 35.0
i1 → **i2**	2	7.25×10^{7}	9.97×10^{7}	1.35×10^{8}	1.80×10^{8}	2.37×10^{8}	3.09×10^{8}	3.98×10^{8}	5.06×10^{8}	6.39×10^{8}	7.98×10^{8}	9.89×10^{8}
i2 → **i1**	1	6.98×10^{6}	9.65×10^{6}	1.31×10^{7}	1.76×10^{7}	2.33×10^{7}	3.04×10^{7}	3.93×10^{7}	5.03×10^{7}	6.37×10^{7}	8.00×10^{7}	9.96×10^{7}
i1 → **i4**	2	5.64×10^{5}	9.52×10^{5}	1.54×10^{6}	2.42×10^{6}	3.68×10^{6}	5.51×10^{6}	7.90×10^{6}	1.12×10^{7}	1.56×10^{7}	2.14×10^{7}	2.89×10^{7}
i4 → **i1**	2	4.34×10^{4}	7.37×10^{4}	1.20×10^{5}	1.90×10^{5}	2.90×10^{5}	4.33×10^{5}	6.31×10^{5}	9.01×10^{5}	1.26×10^{6}	1.74×10^{6}	2.36×10^{6}
i1 → **i6**	2	7.90×10^{7}	1.01×10^{8}	1.29×10^{8}	1.62×10^{8}	2.02×10^{8}	2.49×10^{8}	3.05×10^{8}	3.71×10^{8}	4.48×10^{8}	5.37×10^{8}	6.40×10^{8}
i6 → **i1**	1	4.43×10^{10}	5.22×10^{10}	6.11×10^{10}	7.10×10^{10}	8.20×10^{10}	9.39×10^{10}	1.07×10^{11}	1.21×10^{11}	1.57×10^{11}	1.53×10^{11}	1.71×10^{11}
i2 → **i3**	1	1.16×10^{7}	1.66×10^{7}	2.33×10^{7}	3.21×10^{7}	4.36×10^{7}	5.84×10^{7}	7.72×10^{7}	1.01×10^{8}	1.30×10^{8}	1.67×10^{8}	2.11×10^{8}
i3 → **i2**	2	2.69×10^{6}	3.83×10^{6}	5.35×10^{6}	7.36×10^{6}	9.98×10^{6}	1.33×10^{7}	1.76×10^{7}	2.29×10^{7}	2.96×10^{7}	3.77×10^{7}	4.77×10^{7}
i3 → **i5**	2	4.17×10^{9}	4.59×10^{9}	5.00×10^{9}	5.53×10^{9}	6.04×10^{9}	6.59×10^{9}	7.17×10^{9}	7.79×10^{9}	8.44×10^{9}	9.13×10^{9}	9.85×10^{9}
i5 → **i3**	1	9.36×10^{9}	1.05×10^{10}	1.18×10^{10}	1.31×10^{10}	1.46×10^{10}	1.62×10^{10}	1.80×10^{10}	1.99×10^{10}	2.19×10^{10}	2.41×10^{10}	2.64×10^{10}
i3 → **i6**	2	6.51×10^{2}	1.31×10^{3}	2.46×10^{3}	4.37×10^{3}	7.38×10^{3}	1.20×10^{4}	1.89×10^{4}	2.88×10^{4}	4.28×10^{4}	6.21×10^{4}	8.84×10^{4}
i6 → **i3**	1	1.63×10^{7}	3.03×10^{7}	5.23×10^{7}	8.55×10^{7}	1.34×10^{8}	2.02×10^{8}	2.93×10^{8}	4.16×10^{8}	5.76×10^{8}	7.82×10^{8}	1.03×10^{9}
i3 → **i7**	1	2.67×10^{4}	3.99×10^{4}	5.83×10^{4}	8.34×10^{4}	1.17×10^{5}	1.61×10^{5}	2.19×10^{5}	2.93×10^{5}	3.87×10^{5}	5.04×10^{5}	6.50×10^{5}
i7 → **i3**	1	1.61×10^{9}	2.26×10^{9}	3.10×10^{9}	4.16×10^{9}	5.50×10^{9}	7.15×10^{9}	9.17×10^{9}	1.16×10^{10}	1.45×10^{10}	1.80×10^{10}	2.20×10^{10}
i4 − H_2	1	0	0	5.20×10^{1}	2.01×10^{2}	6.23×10^{2}	1.65×10^{3}	3.86×10^{3}	8.26×10^{3}	1.64×10^{4}	3.07×10^{4}	5.46×10^{4}
i6 → **i7**	1	6.48×10^{10}	7.01×10^{10}	7.56×10^{10}	8.13×10^{10}	8.73×10^{10}	9.32×10^{10}	9.94×10^{10}	1.06×10^{11}	1.12×10^{11}	1.19×10^{11}	1.26×10^{11}
i7 → **i6**	1	7.77×10^{10}	8.58×10^{10}	9.45×10^{10}	1.04×10^{11}	1.13×10^{11}	1.23×10^{11}	1.34×10^{11}	1.45×10^{11}	1.57×10^{11}	1.69×10^{11}	1.81×10^{11}
i7 → **i8**	1	1.51×10^{13}	1.53×10^{13}	1.54×10^{13}	1.55×10^{13}	1.57×10^{13}	1.59×10^{13}	1.60×10^{13}	1.62×10^{13}	1.63×10^{13}	1.64×10^{13}	1.66×10^{13}
i8 → **i7**	1	4.86×10^{12}	4.91×10^{12}	4.95×10^{12}	5.00×10^{12}	5.04×10^{12}	5.09×10^{12}	5.13×10^{12}	5.17×10^{12}	5.21×10^{12}	5.25×10^{12}	5.29×10^{12}
i2 − H	1	1.25×10^{1}	1.78×10^{2}	1.06×10^{3}	4.15×10^{3}	1.29×10^{4}	3.42×10^{4}	8.06×10^{4}	1.62×10^{5}	3.11×10^{5}	5.66×10^{5}	9.70×10^{5}
i3 − H	2	1.65×10^{1}	2.06×10^{2}	1.13×10^{3}	4.14×10^{3}	1.19×10^{4}	2.93×10^{4}	6.51×10^{4}	1.33×10^{5}	2.53×10^{5}	4.56×10^{5}	7.78×10^{5}
i4 − H	2	5.13×10^{1}	6.17×10^{2}	3.24×10^{3}	1.16×10^{4}	3.30×10^{4}	7.99×10^{4}	1.74×10^{5}	3.48×10^{5}	6.55×10^{5}	1.17×10^{6}	2.01×10^{6}
i5 − H	1	0	0	0	1.16×10^{1}	2.17×10^{2}	1.04×10^{3}	3.47×10^{3}	9.44×10^{3}	2.21×10^{4}	4.60×10^{4}	8.92×10^{4}

[a] Reaction path degeneracy.

TABLE 3: Branching Ratios (%) of Various Products of the C_3 + C_2H_2 Reaction Calculated for Collision Energies of 25−35 Kcal/mol

E_c (kcal/mol)	*1*-C_5H + H (from **i2**)	*1*-C_5H + H (from **i3**)	*1*-C_5H + H (from **i4**)	*1*-C_5H + H (total)	HC_2C_3 + H from **i5**)	*1*-C_5 + H_2
25.0	8.429	48.837	42.734	100.0	0	0
26.0	9.726	49.239	41.035	100.0	0	0
27.0	10.623	49.833	38.919	99.375	0	0.624
28.0	11.540	50.718	37.036	99.294	0.060	0.646
29.0	12.564	51.202	35.183	98.949	0.385	0.665
30.0	13.654	51.714	33.201	98.569	0.747	0.684
31.0	14.802	52.861	30.536	98.199	1.123	0.678
32.0	14.949	54.536	28.328	97.813	1.515	0.673
33.0	15.459	55.716	26.294	97.469	1.872	0.659
34.0	15.973	56.853	24.361	97.187	2.175	0.638
35.0	16.364	57.798	22.744	96.906	2.476	0.617

than $C_3 + C_2H_2$. On the other hand, these results imply that the c-$C_3H_2 + C_2(^1\Sigma_g^+)$ and $C_3H + C_2H$ reactions can exothermically produce $C_5H + H$ or $C_3 + C_2H_2$.

Rate Constants and Product Branching Ratios. Rate constants for unimolecular reactions of isomerization and dissociation of various singlet C_5H_2 isomers involved in the $C_3 + C_2H_2$ reaction (starting from intermediate **i1**) were calculated using microcanonical RRKM theory and VTST and are collected in Table 2. The available internal energy for each isomer was taken as the energy of chemical activation in the reaction plus collision energy, E_c, assuming that the major fraction of collision energy will be converted into internal vibrational energy. Since the energy threshold to produce the most favorable l-$C_5H + H$ product is ~24.4 kcal/mol, E_c values were varied from 25.0 to 35.0 kcal/mol with a step of 1 kcal/mol. One can see that the C_5H_2 isomerization rate constants are in general significantly higher than the rate constants for H or H_2 elimination. Therefore, we can expect the relative yields of various products to be controlled by the dissociation rate constants. The rate constants for the formation of l-$C_5H + H$ are calculated to be much higher (by 2−3 orders of magnitude) than those for the steps leading to the cyclic HC_2C_3 structure and to $C_5 + H_2$. The linear C_5H isomer can be formed from **i2**, **i3**, and **i4**, whereas the rate constants for the H loss from these isomers are comparable. Here the H loss from **i4** is 2−3 times faster than from **i2** and **i3**. However, the additional factor controlling relative yields of l-$C_5H + H$ from the **i2**, **i3**, and **i4** isomers is relative concentrations of these precursors.

The calculated branching ratios of l-$C_5H + H$, $HC_2C_3 + H$, and $C_5 + H_2$ as well as relative yields of the linear C_5H isomers produced from **i2**, **i3**, and **i4** are collected in Table 3. One can see that l-$C_5H + H$ are by far the dominant reaction products at all collision energies considered here. They are exclusive products at $E_c = 25-26$ kcal/ mol and at the highest collision energy of 35 kcal/mol their yield is still ~97%. Most of the linear C_5H products are formed by H elimination from pentadiynylidene **i3**; the relative yield increases from ~49% at $E_c = 25$ kcal/mol to ~58% at $E_c = 35$ kcal/ mol. The second important precursor of l-$C_5H + H$ is pentatetraenylidene **i4**; the branching ratio of these products formed from **i4** decreases from 43% to 23% as collision energy rises. Ethynylpropadienylidene **i2** is a relatively minor precursor of linear C_5H with the branching ratio varying from 8% to 16%. The yield of the cyclic C_5H isomer HC_2C_3 increases to about 2% at the highest collision energy, whereas only trace amounts of $C_5 + H_2$, 0.6−0.7%, can be formed in this reaction if it follows statistical behavior.

Conclusions

Ab initio calculations of PES for the $C_3(^1\Sigma_g^+) + C_2H_2(^1\Sigma_g^+)$ reaction demonstrate that this reaction starts from the formation of the 3-(didehydrovinylidene)cyclopropene intermediate **i1** or the five-member ring structure **i7** overcoming sizable entrance barriers of 7.6 and 13.8 kcal/mol, respectively. **i1** can rearrange to the other C_5H_2 intermediates including ethynylpropadienylidene **i2**, singlet pentadiynylidene **i3**, pentatetraenylidene **i4**, ethynylcyclopropenylidene **i5**, and four- and five-member ring isomers **i6**, **i7**, and **i8**, by ring closure and ring opening processes and hydrogen migrations. Intermediates **i2**, **i3**, and **i4** can lose a hydrogen atom to produce the most stable linear isomer of C_5H. Alternatively, H elimination from a cyclic carbon atom in **i5** leads to formation of the second most stable cyclic C_5H isomer, HC_2C_3. 1,1-H_2 loss from pentatetraenylidene **i4** results in the linear pentacarbon product C_5. All the product channels are found to be endothermic, by 24.5, 27.2, and 4.0 kcal/mol for l-$C_5H + H$, $HC_2C_3 + H$, and l-$C_5 + H_2$, respectively. Whereas the H elimination pathways occur without exit barriers, the H_2 loss from **i4** proceeds via a tight transition state residing 26.4 kcal/mol above the $C_3 + C_2H_2$ reactants. These results indicate that the characteristic energy threshold for the reaction under single collision conditions should be in the range of 24−25 kcal/mol. The existence of such a high-energy threshold for the $C_3 + C_2H_2 \rightarrow C_5H + H$ reaction means that although tricarbon molecules can react with acetylene to form l-C_5H in high-temperature combustion flames, this reaction is blocked in cold molecular clouds where the molecules have averaged translational temperatures of about 10 K.

Product branching ratios calculated using RRKM and VTST theories for collision energies between 25 and 35 kcal/mol show that l-$C_5H + H$ are the dominant reaction products. Their relative yield slightly decreases from 100% at $E_c = 25$ kcal/mol to ~97% at the highest collision energy. Most of the l-$C_5H + H$ products are formed either from the **i3** or **i4** intermediates. $HC_2C_3 + H$ and l-$C_5 + H_2$ could be only minor products and their branching ratios do not exceed 2.5% and 0.7%, respectively.

The ethynylcyclopropenylidene isomer **i5** is calculated to be the most stable C_5H_2 species. At our most accurate CCSD(T)/CBS level, it lies 1.8−2.3 kcal/mol lower in energy than triplet pentadiynylidene **i3t**, which was earlier[21] predicted to be the most stable C_5H_2 isomer. The other C_5H_2 local minima are separated from **i5** and **i3t** by significant energy gaps of at least ~13 kcal/mol and larger.

Acknowledgment. This work was funded by the Chemical Sciences, Geosciences and Biosciences Division, Office of Basic Energy Sciences, Office of Sciences of the U.S. Department of Energy (Grant No. DE-FG02-04ER15570 to FIU and Grant No. DE-FG02-03ER15411 to the University of Hawaii).

References and Notes

(1) *Faraday Discuss.* **2001**, *119*, *Combustion Chemistry: Elementary Reactions to Macroscopic Processes*.

(2) (a) Kern, R. D.; Xie, K.; Chen, H. *Combust. Sci. Technol*. **1992**, *85*, 77. (b) Kiefer, J. H.; Sidhu, S. S.; Kern, R. D.; Xie, K.; Chen, H.; Harding, L. B. *Combust. Sci. Technol*. **1992**, *82*, 101. (c) Baukal, C. E. *Oxygen-Enhanced Combustion*; CRS Press: New York, 1998.

(3) (a) Appel, J.; Bockhorn, H.; Frenklach, M. *Combust. Flame* **2000**, *121*, 122. (b) Kazakov, A.; Frenklach, M. *Combust. Flame* **1998**, *114*, 484. (c) Kazakov, A.; Frenklach, M. *Combust. Flame* **1998**, *112*, 270. (d) Vereecken, L.; Bettinger, H. F.; Peeters, J. *Phys. Chem. Chem. Phys.* **2002**, *4*, 2019. (e) Ehrenfreund, P.; Charnley, S. B. *Annu. Rev. Astron. Astrophys.* **2000**, *38*, 427. (f) Richter, H.; Mazyar, O. A.; Sumathi, R.; Green, W. H.; Howard, J. B.; Bozzelli, J. W. *J. Phys. Chem. A* **2001**, *105*, 1561.

(4) Kaiser, R. I.; Le, T. N.; Nguyen, T. L.; Mebel, A. M.; Balucani, N.; Lee, Y. T.; Stahl, F.; Schleyer, P. v. R.; Schaefer, H. F., III *Faraday Discuss.* **2001**, *119*, 51.

(5) (a) Minh, Y. C.; Dishoeck, E. F. *Astrochemistry − From Molecular Clouds to Planetary Systems*; ASP Publisher: San Francisco, 2000. (b) *Faraday Discuss.* **1998**, *109*, *Chemistry and Physics of Molecules and Grains in Space*. (c) Fraser, H. J.; McCoustra, M. R. S.; Williams, D. A. *Astron. Geophys.* **2002**, *43*, 10. (d) Kaiser, R. I.; Ochsenfeld, C.; Stranges, D.; Head-Gordon, M.; Lee, Y. T. *Faraday Discuss.* **1998**, *109*, 183. (e) Chiong, C. C.; Asvany, O.; Balucani, N.; Lee, Y. T.; Kaiser, R. I. In *Proceedings of the 8th Asia-Pacific Physics Conference, APPC*, Taipei, Taiwan, Aug 7−10, 2000; World Scientific Press: Singapore, 2001; p 167. (f) Kaiser, R. I.; Balucani, N. *Int. J. Astrobiol.* **2002**, *1*, 15.

(6) Gu, X.; Guo, Y.; Zhang, F.; Mebel, A. M.; Kaiser, R. I. *Faraday Disc.* **2006**, *133*, 245.

(7) (a) Kaiser, R. I.; Balucani, N.; Charkin, D. O.; Mebel, A. M. *Chem. Phys. Lett.* **2003**, *382*, 112. (b) Gu, X.; Guo, Y.; Mebel, A. M.; Kaiser, R. I. *J. Phys. Chem. A* **2006**, *110*, 11265. (c) Guo, Y.; Kislov, V. V.; Gu, X.; Zhang, F.; Mebel, A. M.; Kaiser, R. I. *Astrophys. J.* **2006**, *653*, 1577.

(8) (a) Mebel, A. M.; Kaiser, R. I.; Lee, Y. T. *J. Am. Chem. Soc.* **2000**, *122*, 1776. (b) Balucani, N.; Mebel, A. M.; Lee, Y. T.; Kaiser, R. I. *J. Phys. Chem. A* **2001**, *105*, 9813. (c) Mebel, A. M.; Kislov, V. V.; Kaiser,

R. I. *J. Chem. Phys.* **2006**, *125*, 133113. (d) Gu, X.; Guo, Y.; Zhang, F.; Mebel, A. M.; Kaiser, R. I. *Chem. Phys.*, submitted for publication.

(9) (a) Mebel, A. M.; Kislov, V. V.; Kaiser, R. I. *J. Phys. Chem. A* **2006**, *110*, 2421. (b) Guo, Y.; Gu, X.; Zhang, F.; Mebel, A. M.; Kaiser, R. I. *J. Phys. Chem. A* **2006**, *110*, 10699.

(10) Gu, X.; Guo, Y.; Zhang, F.; Mebel, A. M.; Kaiser, R. I. *Chem. Phys. Lett.* **2007**, *436*, 7.

(11) Guo, Y.; Gu, X.; Zhang, F.; Mebel, A. M.; Kaiser, R. I. *Phys. Chem. Chem. Phys.* [Online early access]. DOI: 10.1039/b618179a. Published Online: 2007.

(12) Vrtilek, J. M.; Gottlieb, C. A.; Thaddeus, P. *Astrophys. J.* **1987**, *314*, 716.

(13) Cooper, D. L.; Murphy, S. C. *Astrophys. J.* **1988**, *333*, 482.

(14) Thaddeus, P.; Gottlieb, C. A.; Mollaaghababa, R.; Vrtilek, J. M. *J. Chem. Soc., Faraday Trans.* **1993**, *89*, 2125.

(15) McCarthy, M. C.; Travers, M. J.; Kovacs, A.; Chen, W.; Novick, S. E.; Gottlieb, C. A.; Thaddeus, P. *Science* **1997**, *275*, 518.

(16) Travers, M. J.; McCarthy, M. C.; Gottlieb, C. A.; Thaddeus, P. *Astrophys. J.* **1997**, *483*, L135.

(17) Fulara, J.; Freivogel, P.; Forney, D.; Maier, J. P. *J. Chem. Phys.* **1995**, *103*, 8805.

(18) Parent, D. C. *J. Am. Chem. Soc.* **1990**, *112*, 5966.

(19) Fan, Q.; Pfeiffer, G. V. *Chem. Phys. Lett.* **1989**, *162*, 472.

(20) Maluendes, S. A.; McLean, A. D. *Chem. Phys. Lett.* **1992**, *200*, 511.

(21) Seburg, R. A.; McMahon, R. J.; Stanton, J. A.; Gauss, J. *J. Am. Chem. Soc.* **1997**, *119*, 10838.

(22) (a) Bell, M. B.; Feldman, P. A.; Watson, J. K. G.; McCarthy, M. C.; Travers, M. J.; Gottlieb, C. A.; Thaddeus, P. *Astrophys. J.* **1999**, *518*, 740. (b) McCarthy, M. C.; Travers, M. J.; Kovacs, A.; Gottlieb, C. A.; Thaddeus, P. *Astrophys. J., Suppl. Ser.* **1997**, *113*, 105. (c) McCarthy, M. C.; Chen, W.; Travers, M. J.; Thaddeus, P. *Astrophys. J., Suppl. Ser.* **2000**, *129*, 611.

(23) Cernicharo, M.; Kahane, C.; Gómez-González, J.; Guélin, M. *Astron. Astrophys.* **1986**, *164*, L1.

(24) Gottlieb, C. A.; Gottlieb, E. W.; Thaddeus, P. *Astron. Astrophys.* **1986**, *164*, L5.

(25) Ding, H.; Pino, T.; Güthe, F.; Maier, J. P. *J. Chem. Phys.* **2002**, *117*, 8362.

(26) Crawford, T. D.; Stanton, J. F.; Saeh, J. C.; Schaefer, H. F., III *J. Am. Chem. Soc.* **1999**, *121*, 1902.

(27) Becke, A. D. *J. Chem. Phys.* **1993**, *98*, 5648.

(28) Lee, C.; Yang, W.; Parr, R. G. *Phys. Rev. B* **1988**, *37*, 785.

(29) Gonzales, C.; Schlegel, H. B. *J. Chem. Phys.* **1989**, *90*, 2154.

(30) (a) Purvis, G. D.; Bartlett, R. J. *J. Chem. Phys*. **1982**, *76*, 1910. (b) Scuseria, G. E.; Janssen, C. L.; Schaefer, H. F., III *J. Chem. Phys*. **1988**, *89*, 7382. (c) Scuseria, G. E.; Schaefer, H. F. *J. Chem. Phys*. **1989**, *90*, 3700; Pople, J. A.; Head-Gordon, M.; Raghavachari, K. *J. Chem. Phys.* **1987**, *87*, 5968.

(31) Dunning, T. H., Jr. *J. Chem. Phys.* **1989**, *90*, 1007.

(32) (a) Peterson, K. A.; Woon, D. E.; Dunning, T. H., Jr. *J. Chem. Phys.* **1994**, *100*, 7410. (b) Woon, D. E.; Dunning, T. H., Jr. *J. Chem. Phys*. **1994**, *100*, 2975. (c) Xantheas, S. S.; Dunning, T. H., Jr. *J. Phys. Chem.* **1993**, *97*, 18. (d) Peterson, K. A.; Dunning, T. H., Jr. *J. Chem. Phys.* **1995**, *102*, 3032.

(33) Peterson, K. A.; Dunning, T. H., Jr. *J. Chem. Phys.* **1995**, *99*, 3898.

(34) Frisch, M. J.; Trucks, G. W.; Schlegel, H. B.; Scuseria, G. E.; Robb, M. A.; Cheeseman, J. R.; Zakrzewski, V. G.; Montgomery, J. A., Jr.; Stratmann, R. E.; Burant, J. C.; Dapprich, S.; Millam, J. M.; Daniels, A. D.; Kudin, K. N.; Strain, M. C.; Farkas, O.; Tomasi, J.; Barone, V.; Cossi, M.; Cammi, R.; Mennucci, B.; Pomelli, C.; Adamo, C.; Clifford, S.; Ochterski, J.; Petersson, G. A.; Ayala, P. Y.; Cui, Q.; Morokuma, K.; Malick, D. K.; Rabuck, A. D.; Raghavachari, K.; Foresman, J. B.; Cioslowski, J.; Ortiz, J. V.; Baboul, A. G.; Stefanov, B. B.; Liu, G.; Liashenko, A.; Piskorz, P.; Komaromi, I.; Gomperts, R.; Martin, R. L.; Fox, D. J.; Keith, T.; Al-Laham, M. A.; Peng, C. Y.; Nanayakkara, A.; Gonzalez, C.; Challacombe, M.; Gill, P. M. W.; Johnson, B.; Chen, W.; Wong, M. W.; Andres, J. L.; Head-Gordon, M.; Replogle, E. S.; Pople, J. A. *Gaussian 98*, Revision A.9; Gaussian, Inc.: Pittsburgh, PA, 1998.

(35) Amos, R. D.; Bernhardsson, A.; Berning, A.; Celani, P.; Cooper, D. L.; Deegan, M. J. O.; Dobbyn, A. J.; Eckert, F.; Hampel, C.; Hetzer, G.; Knowles, P. J.; Korona, T.; Lindh, R.; Lloyd, A. W.; McNicholas, S. J.; Manby, F. R.; Meyer, W.; Mura, M. E.; Nicklass, A.; Palmieri, P.; Pitzer, R.; Rauhut, G.; Schütz, M.; Schumann, U.; Stoll, H.; Stone, A. J.; Tarroni, R.; Thorsteinsson, T.; Werner, H.-J. *MOLPRO*, version 2002.6; University of Birmingham: Birmingham, U.K., 2003.

(36) Eyring, H.; Lin, S. H.; Lin, S. M. *Basic Chemical Kinetics*; Wiley: New York, 1980.

(37) Robinson, P. J.; Holbrook, K. A. *Unimolecular Reactions*; Wiley: New York, 1972.

(38) Steinfield, J. I.; Francisco, J. S.; Hase, W. L. *Chemical Kinetics and Dynamics*; Prentice Hall: Engelwood Cliffs, NJ, 1999.